ITERATIVE DISCRETE STEERING
OF THREE-DIMENSIONAL RECONSTRUCTIONS FROM
X-RAY IMAGES WITH LIMITED ANGLE

Anja Frost, Eike Renners and Michael Hötter

Institut für Innovationstransfer, University of Applied Sciences and Arts, Ricklinger Stadtweg 120, Hannover, Germany

Keywords: Computer Tomography, CT, Discrete Tomography, DT, X-ray, Emission Data, Limited Data Problem, Three Dimensional Image Reconstruction, Algebraic Reconstruction Technique (ART), Binary Steering, Evaluation, Probability Calculus, Accuratio.

Abstract: Computer Tomography is aimed to calculate a three dimensional reconstruction of the inside of an object from series of X-ray images. This calculation corresponds to the solution of a system of linear equations, in which the equations arise from the measured X-rays and the variables from the voxels of the reconstruction volume, or more precisely, their density values. Unfortunately, some applications do not supply enough equations. In that case, the system is underdetermined. The reconstructed object, as only estimated, seems to be stretched. As there are a few voxels, that are already representing the object true to original, it is possible to exclude these variables from the system of equations. Then, the number of variables decreases. Ideally, the system gets solvable. In this paper we concentrate on the detection of all good reconstructed voxels i.e. we introduce a quality measure, called *Accuratio*, to evaluate the volume voxel by voxel. In our experimental results we show the reliability of *Accuratio* by applying it to an iterative reconstruction algorithm. In each iteration step the whole volume is evaluated, voxels with high *Accuratio* are excluded and the new system of equations is reconstructed again. Steadily the reconstructed object becomes "destretched".

1 INTRODUCTION

First and foremost, Computer Tomography was introduced for clinical diagnostics. Nowadays, it is also used for quality assurance in the production and maintenance of any object. As it generates a three dimensional reconstruction of the inside of the object from series of X-ray images, inner structures such as casting defects or cold soldered connections become visible. Moreover, exact measurements of the shape are feasible. But the very use in quality assurance demands reconstructions that are absolutely true to original. To calculate such reconstructions, it is necessary to provide many X-ray images from different angles of vision. Ideally, the object is turned through 360° while x-raying.

In some applications it is not possible to turn the object through 360°. For example, if the shape is bulky and stops the rotation in the computer tomography scanner, then the number of X-ray images is reduced. Mathematically speaking, the reconstruction problem is underdetermined. The reconstructed volume can only be estimated. For the most voxels this estimation differs drastically from the target. The object seems to be stretched (shown in Figure 1).
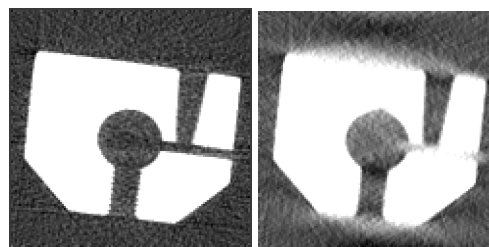

Figure 1: Cross sections through the reconstructed volume from a series of X-ray images spanning 360° (left image) and 135° (right image).

An underdetermined system of equations can not be solved in principle. But including a priori knowledge that does not arise from the measurement can improve the reconstruction quality. There are two types of a priori knowledge; knowledge about the shape, and knowledge about the materials the x-rayed object consists of, i.e. the density of each

material. An abundance of approaches exists for both types.

Most of all solutions that deal with knowlege about the shape fit a parametric model to the reconstructed object. They get useful results, as shown for example by Benameur et al. (2003) or Sadowsky et al. (2011). Others handle fragmentary knowledge about the shape demanding smoothness of the surface or similar, and usually combine knowledge about the material densities (Varga, Balázs and Nagy, 2010).

It becomes more difficult to improve the reconstruction of any object due to the sheer knowledge about the material densities. Some approaches achieve passable results for objects that consist of one material only. Then, the reconstruction problem is a binary decision between object and air. But the algorithms get unreliable if the object is composed of several materials and x-rayed with limited angle. Herman and Kuba published a compendium of these works in 2007.

In our approach, we introduce a new quality measure to evaluate a volume voxel by voxel including a priori knowledge about the materials, no matter the number of different materials. By evaluating, voxels that are representing the target true to original get detected. In a second step, we exclude the detected voxels from the system of equations. This means, the number of variables decreases. The reconstruction problem, which was once underdetermined, becomes solvable.

In Section 2.1 we introduce the basic notation and give an overview about conventional reconstruction techniques. Then, in Section 2.2 we enter into the question how to decrease the number of variables. In Section 3 the evaluation step is described. We present and discuss our experimental results in Section 4. A few remarks conclude the paper.

2 RECONSTRUCTION TECHNIQUES

2.1 Foundations

Physically, the grey value y_i of pixel i in an measured X-ray image is equal to the line integral of the density $x(l)$ along the ray path l.

$$y_i = \int x(l)\, dl \qquad (1)$$

To calculate a reconstruction of the x-rayed

object in a quantised grid the equation (1) changes into equation (2).

$$y_i = \sum_{n=1}^{N} w_{ni} x_n \qquad (2)$$

Here, N is the number of voxels in the whole volume, x_n represents the density of voxel n, and w_{ni} describes the contribution of the nth voxel to the ith measurement. Figure 2 shows a ray path through the volume. Voxels with $w_{ni} \neq 0$ are marked with a red outline.
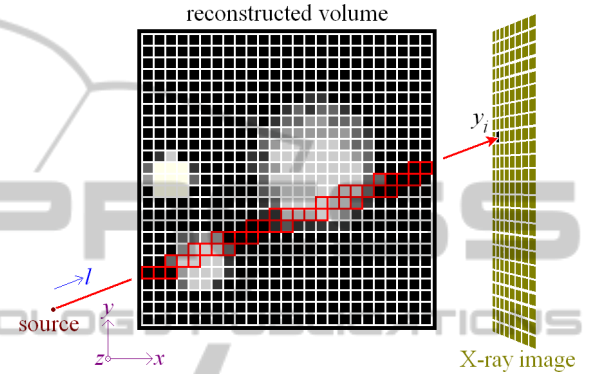

Figure 2: X-ray in a regular grid.

There are several techniques to calculate the densities x_n from the measured X-rays y_i, listed very comprehensively in (Kak and Slaney, 1988). These techniques can be divided into two categories: On the one hand, there are analytical methods, which involve all X-ray images to generate one reconstruction. On the other, there are iterative methods that approach the solution step by step. In each step a correction for the current reconstruction is calculated.

One of the most frequently referred iterative reconstruction algorithms in highly topical works is ART, first published by Gordon, Bender and Herman (1970), recently adapted to GPU-based calculation and sophisticated by Xu and Müller (2007). As we adapt this technique to our work, we explain it more detailed.

In ART, the differences $y_i - \sum w_{ni} x_n$ of all measurements i are minimised by applying the Kaczmarz method (Kunze, 2007). This leads to the correction equation (3) for the density x_j of a voxel j and for iteration number $k+1$.

$$x_j^{(k+1)} = x_j^{(k)} + \frac{y_i - \sum_{n=1}^{N} w_{ni} x_n^{(k)}}{\sum_{n=1}^{N} w_{ni} w_{ni}} \cdot w_{ji} \qquad (3)$$

As long as $y_i \neq \sum w_{ni}x_n$, the difference $y_i - \sum w_{ni}x_n$ is divided by the number of voxels that are part of the ray i ($w_{ni} \neq 0$), and distributed uniformly among these voxels. In this way, after adding in accordance with (3), the difference $y_i - \sum w_{ni}x_n$ is zero. Equation (2) is met, but for the current ray i only.

2.2 Vary the Number of Variables

In the following, $A = \{1, 2, 3, ..., N\}$ is the set of all voxels, strictly speaking their indices. B is a subset of A and contains all bad reconstructed voxels i.e. the remaining variables. The equation (2) can be expressed by (4).

$$y_i = \sum_{n \in B} w_{ni}x_n + \sum_{n \notin B} w_{ni}x_n \qquad (4)$$

Based on (4), the ART correction equation for any voxel $j \in B$ changes into

$$x_j^{(k+1)} = x_j^{(k)} + \frac{y_i - \sum_{n \in A} w_{ni}x_n^{(k)}}{\sum_{n \in B} w_{ni}w_{ni}} \cdot w_{ji} \qquad (5)$$

and only for $j \in B$ the update is executed.

Now, the difference $y_i - \sum w_{ni}x_n \neq 0$ is distributed among the bad reconstructed voxels only, i.e. exactly the voxels that have produced the difference.

The basic idea of excluding good reconstructed voxels from the system of equations is already mentioned by Batenburg and Sijbers (2007). In contrast to our topic, they work on the problem of limited data, which yields reconstructions that are slightly deformed in all directions. In our approach we use a novel quality measure in the evaluation step, better fitted to the problem of limited angle i.e. extremely stretched reconstructions.

3 EVALUATION STEP

3.1 Include A Priori Knowledge

There are many ways of including a priori knowledge about the materials of which the X-rayed object consists into its reconstruction. Some present works use a conventional reconstruction technique (according to Section 2.1), and afterwards put in a priori knowledge. In the simplest case, for example in (Censor 2001), the reconstructed density x_n is discretised via thresholding.

Others, such as Kuba, Ruskó, Rodek and Kiss (2005) extend the cost function with an additive term which includes a priori knowledge. For our aim to evaluate the reconstruction, we pursue a related strategy: For every voxel j the reconstructed density x_j is replaced successively with each predefined material density m_d. For each inserted material density and for each X-ray i crossing the selected voxel the mean square deviation between y_i and $\sum w_{ni}x_n$ is calculated. The sum of all mean square deviations, normalised to the number of rays I, is called density error $f_j(m_d)$ (6).

$$f_j(m_d) = \frac{\sum_{i=1}^{I} \left(y_i - \sum_{n \in A} w_{ni}x_n + w_{ji}x_j - w_{ji}m_d \right)^2}{I} \qquad (6)$$

The higher the support of the measurements for a material density m_d is (or, metaphorically speaking, the more X-rays the material density m_d prefer), the smaller will be the density error $f_j(m_d)$.

3.2 Probability Modelling

The density errors $f_j(m_d)$ already provide a basis for the selection of the most probable material m_d (q.v. Frost and Hötter (2010)). But in order to classify a voxel, we need a quality measure that is independent of parameters such as the object size and enables a quantitative evaluation of the reconstruction quality. Therefore, we convert the density error $f_j(m_d)$ into a probability $p_j(m_d)$: a probability of existence of the material m_d at the position j. The conversion takes three constraints into account: $p_j(f_j=0) = 1$, $0 \leq p_j(f_j) \leq 1$ and $p_j(f_j)$ is strictly monotonic decreasing. The Gaussian function in (7) fulfils the three constraints.

$$p_j(f_j) \sim e^{-\pi \cdot f_j^2} \qquad (7)$$

The output of (7) still depends on the material densities and size of the x-rayed object. In case it is demanded to compare various reconstructions with different objects, the conversion in (7) has to be expanded by a fourth constraint; If two distinct material densities, for example m_d and m_{d+1}, produce density errors $f_j(m_d)$ and $f_j(m_{d+1})$ that are equal in value, it is impossible to come to a decision. Both materials are equiprobable. In this instance the density error is the squared half difference of both material densities and $p_j(f_j = ((m_{d+1} - m_d)/2)^2) = 0.5$. Considering this fourth constraint, we get the conversion formula (8).

$$p_j(f_j) = e^{-\ln 2 \left(\frac{f_j}{((m_{d+1} - m_d)/2)^2} \right)^2} \qquad (8)$$

3.3 Probability Distribution

The probability $p_j(m_d)$ of material density m_d with $d = 1...D$ and D different materials yields a probability distribution. For a good reconstructed voxel j the very density m_d, which was really existing at the position j while x-raying, is supported by the most rays and stands out with a high probability $p_j(m_d)$. For a more inaccurate reconstructed voxel, the rays do not correspond with the preferred material density. In this case, less rays support the real density m_d. The probability $p_j(m_d)$ is lower.

Figure 3 shows exemplarily the probability distributions of two voxels in a reconstructed volume. Voxel g is situated inside of the large sphere and evidently good reconstructed. The probability distribution holds a distinct maximum at material density m_1, which stands for the sphere material. Voxel b is near to the surface. The reconstruction in this area is difficult, because some measurements prefer material density m_1, and others favour the air density m_0. There is no outstanding maximum in the probability distribution.
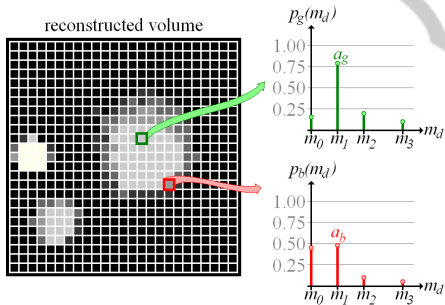

Figure 3: Probability distribution of a good reconstructed voxel g (green coloured) as well as of a bad reconstructed voxel b (red coloured).

3.4 Quality Measure

Now, for each voxel there is a probability distribution which expresses the quality of the reconstruction. For the practical application it is necessary to handle one numerical value instead of a function. Hence, we pick out the maximum of probability distribution $\max(p_j)$, briefly called *Accuratio* a_j, since this maximum already obtains all the information required for quality determining. Figure 4 shows a cross section through the *Accuratio* volume that corresponds to a 135°-reconstruction. The higher the *Accuratio* of a voxel, the lighter the grey is displayed. It becomes visible that *Accuratio* is generally high, except for the falsified areas, where a low *Accuratio* predominates.
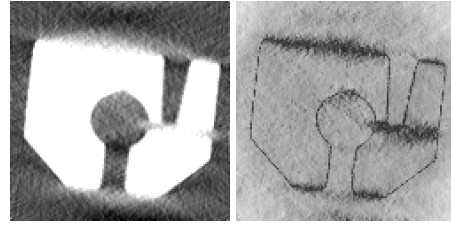

Figure 4: Cross section through the reconstructed volume from a series of X-ray images spanning 135° (left image) and corresponding *Accuratio* (right image).

Binarising the *Accuratio* volume, we distinguish "good" from "bad" reconstructed voxels.

4 EXPERIMENTAL RESULTS

4.1 Algorithm of Discrete Steering

In our experiment we executed the reconstruction algorithm outlined in Figure 5.
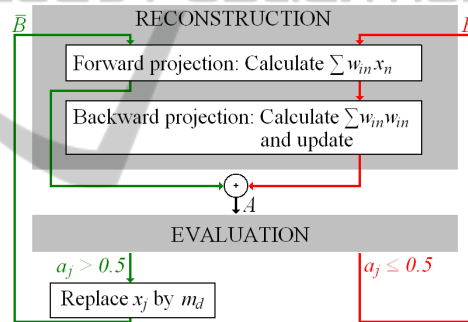

Figure 5: Iteration of Discrete Steering.

At the start, the subset B is equal to A. The whole volume will be reconstructed. When each X-ray image was used for reconstruction once, each voxel is evaluated by our quality measure. Voxels with $a_j > 0.5$ are defined as "good" and excluded from the subset B. Moreover, their reconstructed density x_j is replaced by the most likely material m_d. In this way, the reconstruction is steered into a discrete solution. In the next reconstruction step (according to equation 5), the "good" voxels go into $\sum w_{ni}x_n$, which is also called forward projection. But only the "bad" voxels become reconstructed again.

4.2 Test Objects and Scenes

The experiment deals with one mathematically defined object (A) and one real work piece made of aluminium (B). Object A modelled on a circuit board (Figure 6). Three soldered points (material

Figure 6: Cross section in xy-plane of test object A.

density $m_3 = 2.7$) are situated between two plates ($m_1 = 0.9$). On the top, there is a flat box ($m_2 = 1.8$). From this model we generated 29 X-ray images in a 157° rotation around the z-axis. Each image has the size of 64² pixels. The volume contains 64³ voxels.

Object B we describe as screw-nut. 168 X-ray images on a scale of 168 x 128 pixels were measured in a 360° rotation. The reconstruction of the complete data is shown in Figure 1 (on the left). Afterwards, we limited the angle range to 135°.

The Figures 7 and 8 demonstrate the influence of limited angle on conventional ART as well as the improvements by Discrete Steering. As can be seen, the results of ART are falsified: In Figure 7 (Object A) all horizontal surfaces, such as the plates, are blurred. Hence, the crack between the right soldering and upper plate vanishes completely. In Figure 8 (Object B) the air gap is invisible, too. Additionally, the reconstruction volumes do not change significantly during 8 iterations of ART. At the same time, in each iteration step of Discrete Steering the reconstructed objects converge more and more to the original shape. The first evaluation step already improves the reconstruction. Here, due to the inclusion of a priori knowledge, some falsified areas can be corrected immediately. For example, light artefacts in the air disappear. In case the falsified areas can not be corrected, they show low *Accuratio*s and will be reconstructed again. In the following evaluation steps, the number of bad reconstructed voxels decreases. In Figure 7 the plates get a distinct shape and the crack between the right soldering and upper plate becomes visible. In

Figure 8 the air gap is detected by low *Accuratio*s. To sum up, in the end the reconstructed objects show the rough shape of the original or, at least, an improvement compared to the results of ART.

In 24 test series with varied limited angles from 129° to 157° we recorded the number of correctly discretised voxels while reconstructing. In comparison to ART (with discretisation via thresholding), the Discrete Steering Algorithm performs a faster as well as longer rise, and finally keeps 98 % correctly discretised voxels on average.

5 CONCLUSIONS

We have presented a technique to generate three dimensional reconstructions from X-ray images spanning a limited angle only, i.e. in the first instance the system of equations is underdetermined. By detecting and excluding all good reconstructed voxels from the system of equations, the number of variables decrease and the system gets solvable.

To distinguish "good" from "bad" reconstructed voxels, we have applied the new quality measure *Accuratio*: For each voxel there is calculated a probability distribution of a priori known material density by taking into account all X-rays that are crossing the selected voxel. The better the reconstruction is, the more X-rays prefer the same material and the more the maximum of the distribution increases. If the maximum exceeds 0.5, we define the voxel as "good" assuming that the corresponding material density really existed at the position of the selected voxel while measuring.

We have shown in our experimental results that *Accuratio* is suited to detect "good" and "bad" voxels. The very first evaluation step marks falsified areas or correct them reliably. In the following iterations, the number of bad reconstructed voxels
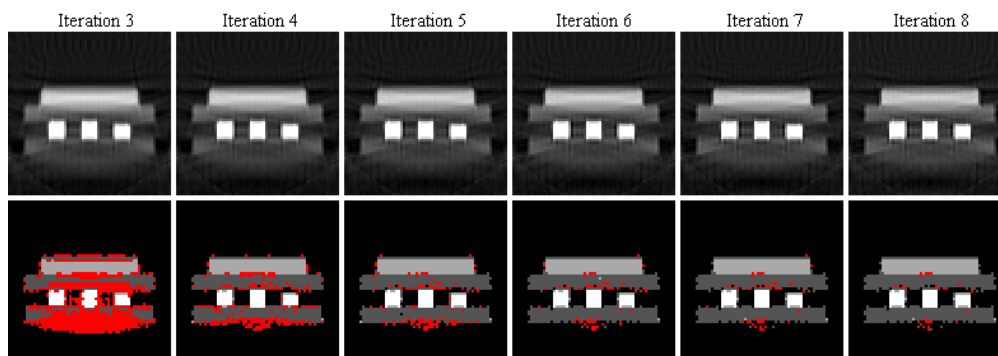

Figure 7: Cross sections through the reconstruction volume of test object A applying conventional ART (upper row) and Discrete Steering (lower row). In the results of Discrete Steering, voxels with $a_j \leq 0.5$ are red marked.
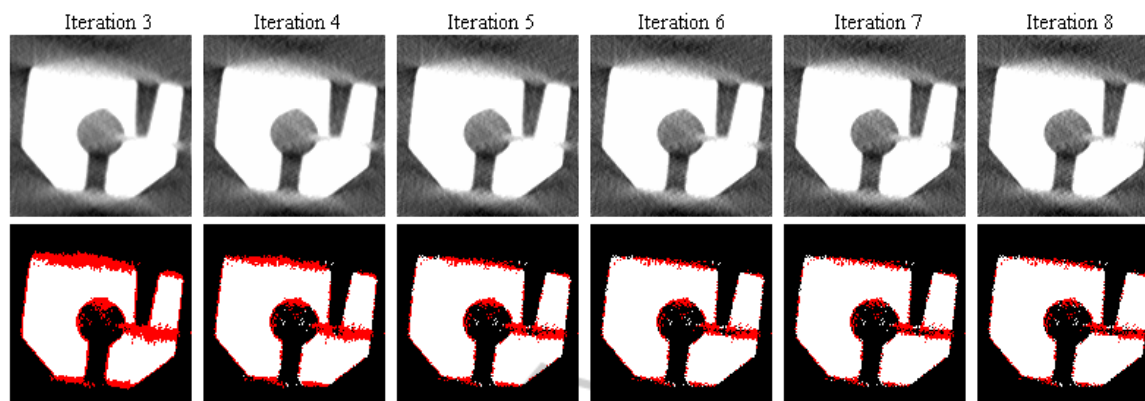
Figure 8: Cross sections through the reconstruction volume of test object B applying conventional ART (upper row) and Discrete Steering (lower row). In the results of Discrete Steering, voxels with $a_j \leq 0.5$ are red marked.

decreases. The over all quality increases. In the end, the reconstructed objects are closer to the original, though a lot of noise appeared. In further works we want to address the problem by separate noise suppression.

REFERENCES

Benameur, S., Mignotte, M., Labelle, H., De Guise, J.A., 2003. A hierarchical statistical modeling approach for the unsupervised 3-D biplanar reconstruction of the scoliotic spine. In *IEEE Transactions of Biomedical Engineering*, 52(12), 2041-2057.

Sadowsky, O., Lee, J., Sutter, E. G., Wall, S. J., Prince, J. L., Taylor, R.H., 2011. Hybrid cone-beam tomographic reconstruction: incorporation of prior anatomical models to compensate for missing data. In *IEEE Transactions on Medical Imaging*, 30(1), 69-83.

Varga, L., Balázs, P., Nagy, A., 2010. Projection selection algorithms for discrete tomography. In *Advanced Concepts for Intelligent Vision Systems*, Springer. pp. 390-401.

Herman, G. T., Kuba, A., 2007. *Advances in discrete tomography and its applications*, Birkhäuser. Bosten.

Kak, A. C., Slaney, M., 1988. *Principles of computerized tomographic imaging*, IEEE Press. New York.

Gordon, R., Bender, R., Herman, G. T., 1970. Algebraic Reconstruction Techniques (ART) for three-dimensional electron microscopy and X-ray photography. In *Journal of Theoretical Biology,* 29(3), pp. 471-481. Elsevier.

Xu, F., Müller, K., 2007. Real-time 3D computed tomographic reconstruction using commodity graphics hardware. In *Physics in Medicine and Biology.* 52, pp. 3405-3419. IOP Publishing.

Kunze, H., 2007. Iterative Rekonstruktion in der medizinischen Bildverarbeitung, Shaker.

Batenburg, K. J., Sijbers, J., 2007. Dart: A Fast Heuristic Algebraic Reconstruction Algorithm for Discrete Tomography. In *Image Processing, 4th IEEE Conference on Image Processing.* doi: 10.1109/ICIP. 2007.4379972

Kuba, A., Ruskó, L., Rodek, L., Kiss, Z., 2005. Preliminary studies of discrete tomography in neutron imaging. In *IEEE Transactions on Nuclear Science.* 52(1), pp. 380-385. IEEE Press.

Censor, Y., 2001. Binary steering in discrete tomography reconstruction with sequential and simultaneous iterative algorithms. In *Linear Algebra and its Applications* (Vol. 339(1-3), pp. 111-124). Elsevier.

Frost, A., Hötter, M., 2010. Discrete Steering: Eine statistisch orientierte Diskretisierung von dreidimensionalen Rekonstruktionen aus Röntgenaufnahmen. In Puente León, F. and Heizmann, M, *Forum Bildverarbeitung: [2. - 3. Dezember 2010 in Regensburg]* (pp. 365-376). KIT Scientific Publishing.